Received: 8 December 2016 | Revised: 30 December 2016 | Accepted: 31 December 2016

DOI 10.1002/aoc.3747

FULL PAPER

WILEY Applied Organometallic Chemistry

Two silver(I) complexes with bis(benzimidazole)-2-oxopropane ligands: Syntheses, crystal structures and DNA binding studies

Shanshan Mao | Kesheng Shen | Xinkui Shi | Yuling Xu | Huilu Wu

School of Chemical and Biological Engineering, Lanzhou Jiaotong University, Lanzhou, Gansu, 730070, People's Republic of China

Correspondence
Huilu Wu, School of Chemical and Biological Engineering, Lanzhou Jiaotong University, Lanzhou, Gansu, 730070, People's Republic of China.
Email: wuhuilu@163.com

Funding information
National Natural Science Foundation of China, Grant/Award Number: 21367017.

Two Ag(I) complexes, $[Ag_2(bobb)_2]\cdot(NO_3)_2$ (**1**) and $[Ag_2(crotonate)_2(aobb)]_n$ (**2**) (bobb =1,3-bis(1-benzylbenzimidazol-2-yl)-2-oxapropane; aobb =1,3-bis(1-allylbenzimidazol-2-yl)-2-oxopropane), have been synthesized and characterized using elemental analysis, electrical conductivities, infrared and UV–visible spectral measurements and single-crystal X-ray diffraction. Complex **1** is binuclear and three-coordinated by two N atoms from two bobb ligands, while complex **2** is a unique metal organic compound with diamond-like multinuclear Ag centers with each Ag bridged by two aobb ligands and two crotonate ions to form one-dimensional single polymer chain structures and extended into two-dimensional frameworks through π–π and intermolecular C─H···O hydrogen bonds. The adjacent Ag(I) centers are bridged by allyl from aobb which is not only a σ-bonding ligand, but also a π-acid ligand. The DNA binding modes of complexes **1** and **2** were investigated using electronic absorption titration, fluorescence spectra and viscosity measurements. The results suggest that the two complexes bind to DNA via an intercalative mode, and their binding affinity for DNA follows the order **2** > **1**. This is due to the chelating effects which can enhance the planar functionality of the metal complexes.

KEYWORDS
Ag(I) complexes, bis(benzimidazole)-2-oxopropane, crystal structure, DNA binding property, syntheses

1 | INTRODUCTION

Benzimidazole derivatives are important constituents in many pharmacologically, catalytically and biologically active compounds, and therefore correspond to significant synthetic targets.[1–3] These benzimidazoles are known for their potential to poison DNA topoisomerases or to stabilize complexes of DNA topoisomerases that ultimately result in strand cleavage.[4] Study of the interaction of transition metal complexes with DNA has been of particular interest to researchers in the field of bioinorganic chemistry.[5–7] Metal complexes binding to nucleic acids are currently investigated because of their utility as DNA structural probes, DNA foot-printing and sequence-specific cleavage agents and potential anticancer drugs.[8] A large number of complexes have been synthesized and explored for their biological activities.[9]

It is well known that Ag(I) is a favorable and well-studied ion for the construction of coordination clusters because of its coordination diversity as well as its positive coordination tendency with various donor atoms.[10–12] The compounds formed by Ag(I) atoms and multi-topic N-donor ligands have attracted great interest for a number of reasons. The soft Ag^+ (d^{10}) ion has been commonly used as a metal center in the construction of coordination polymers.[13] The Ag(I) center has a closed-shell electronic configuration and can adopt diverse coordination numbers from 2 to 8, with no strong energetic preference for any particular geometry,[14,15]

varying from linear to trigonal, tetragonal, square pyramidal, octahedral, and so on. In recent years, researchers have explored silver-, gold- and platinum-based N-heterocyclic carbenes having benzimidazole cores as excellent antitumor and anticancer agents in the form of complexes. Their various biological applications with fewer side effects are now attracting global attention.[16]

In the study reported here, two new complexes, namely $[Ag_2(bobb)_2]\cdot(NO_3)_2$ (**1**) and $[Ag_2(crotonate)_2(aobb)]_n$ (**2**) (bobb =1,3-bis(1-benzylbenzimidazol-2-yl)-2-oxapropane; aobb =1,3-bis(1-allylbenzimidazol-2-yl)-2-oxopropane), were synthesized and characterized. The DNA binding behaviors of the two complexes were investigated.

2 | EXPERIMENTAL

2.1 | Materials and methods

C, H and N elemental analyses were conducted using a Carlo Erba 1106 elemental analyzer. Electrolytic conductance measurements were made with a DDS-11A type conductivity bridge using 10^{-3} M solutions in dimethylformamide (DMF) at room temperature. Infrared (IR) spectra were recorded in the region 400–4000 cm^{-1} with a Nicolet FT-VERTEX 70 spectrometer using KBr pellets. Electronic spectra were recorded with a Lab-Tech UV Bluestar spectrophotometer. ^1H NMR spectra were recorded using a Varian VR 300 MHz spectrometer with teramethylsilane as an internal standard. Fluorescence spectra were recorded with a PerkinElmer LS-45 spectrofluorophotometer. Melting points were determined with an X-4 digital micro melting point apparatus.

Calf thymus DNA (CT-DNA) and ethidium bromide (EB) were obtained from Sigma-Aldrich. All chemicals used for experiments were of analytical grade. Other reagents and solvents were of reagent grade obtained from commercial sources and used without further purification. Tris–HCl buffer, Na_2HPO_4–NaH_2PO_4 buffer and EDTA–Fe(II) solution were prepared using doubly distilled water. Stock solutions of the complexes were prepared in DMF at 3×10^{-3} M. The experiments involving interaction of ligands and complexes with CT-DNA were carried out in doubly distilled buffered water containing 5 mM Tris and 50 mM NaCl and adjusted to pH = 7.2 with hydrochloric acid. A solution of CT-DNA gave a ratio of UV absorbance at 260 and 280 nm of about 1.8–1.9, indicating that the CT-DNA was sufficiently free of protein.[17] The CT-DNA concentration per nucleotide was determined spectrophotometrically by employing an extinction coefficient of 6600 M^{-1} cm^{-1} at 260 nm.[18] Ligands bobb and aobb were synthesized according to a literature method,[19,20] as shown in Scheme 1.

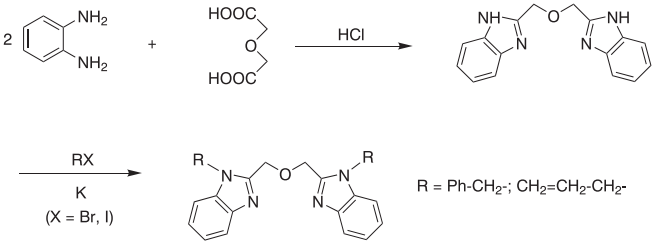

SCHEME 1 Synthetic route for ligands bobb and aobb

2.2 | Synthesis of complexes

2.2.1 | Preparation of $[Ag_2(bobb)_2]$ $(NO_3)_2$ (1)

To a stirred solution of bobb (0.0916 g, 0.20 mmol) in hot MeOH (5 ml) was added $AgNO_3$ (0.0340 g, 0.20 mmol) in MeOH (5 ml) at room temperature for 4 h. This was then filtered and a few drops of acetonitrile added to the colorless filtrate avoiding light. Slow evaporation at room temperature led to block-structure crystals after about 3–5 weeks. Yield 69%; m.p. 283–285 °C (decomp.). Anal. Calcd for $C_{60}H_{52}Ag_2N_{10}O_8$ (%): C, 61.4; H, 4.7; N, 8.9. Found (%): C, 61.5; H, 4.6; N, 9.0. IR (KBr, ν, cm^{-1}): 746 ν(O—Ar), 1043 ν(C—O), 1382 $\nu(NO^{3-})$, 1548 ν(C=N). UV–visible (DMF, λ, nm): 273, 288 nm. Λ_M (DMF, 297 K): 127 S cm^2 mol^{-1}.

2.2.2 | Preparation of $[Ag_2(crotonate)_2(aobb)]_n$ (2)

An ethanol aqueous solution (5 ml) of sodium crotonate (0.0217 g, 0.20 mmol) was added to a ethanol solution (3 ml) of $AgNO_3$ (0.0340 g, 0.20 mmol) and stirred for several minutes until a precipitate was generated. Then aobb (0.0716 g, 0.20 mmol) in ethanol (5 ml) was added and stirred at room temperature for 4 h until the white precipitate disappeared. This was then filtered and a few drops of acetonitrile added to the colorless filtrate avoiding light. Slow evaporation at room temperature led to block-structure crystals after about 3–5 weeks. Yield 71%; m.p. 259–262 °C (decomp.). Anal. Calcd for $C_{30}H_{32}Ag_2N_4O_5$ (%): C, 48.4; H, 4.3; N, 7.5. Found (%): C, 48.3; H, 4.4; N, 7.5. IR (KBr, ν, cm^{-1}): 738 ν(O—Ar), 1053 ν(C—O), 1498 ν(C=N), 1549 ν_{as}(COO), 1402 ν_s(COO). UV–visible (DMF, λ, nm): 280, 288. Λ_M (DMF, 297 K): 8 S cm^2 mol^{-1}.

2.3 | X-ray crystallography

For each complex, a suitable single crystal was mounted on a glass fiber, and the intensity data were collected using a Bruker APEX-II CCD diffractometer with graphite-monochromatized Mo Kα radiation (λ = 0.71073 Å) at 296(2) K. Data reduction and cell refinement were performed using the SAINT suite of

programs.[21] The absorption corrections were made using empirical methods. The structures were solved by direct methods and refined by full-matrix least-squares against F^2 using SHELXTL software.[22] All H atoms were found in difference electron maps and subsequently refined in a riding model approximation with C—H distances ranging from 0.95 to 0.99 Å and $U_{iso}(H) = 1.2U_{eq}(C)$ or $1.5U_{eq}(C_{methyl})$. The crystal data and experimental parameters relevant to the structure determination are listed in Table 1. Selected bond distances and angles are given in Table 2.

2.4 | DNA binding experiments

2.4.1 | Electronic absorption titration

Absorption titration experiments were performed with fixed concentrations of the complexes, while gradually increasing the concentration of CT-DNA. To obtain the absorption spectra, the required amount of CT-DNA was added to both compound and reference solutions to eliminate the absorption of CT-DNA itself. From the absorption titration data, the binding constant (K_b) was determined using the following equation[23]:

$$\frac{[DNA]}{\varepsilon_a-\varepsilon_f} = \frac{[DNA]}{\varepsilon_b-\varepsilon_f} + \frac{1}{K_b(\varepsilon_b-\varepsilon_f)}$$

where [DNA] is the concentration of CT-DNA in base pairs, ε_a corresponds to the observed extinction coefficient (A_{obs}/[M]), ε_f corresponds to the extinction coefficient of the free compound, ε_b is the extinction coefficient of the complex when fully bound to CT-DNA and K_b is the intrinsic binding constant. The ratio of slope to intercept of a plot of [DNA]/($\varepsilon_a - \varepsilon_f$) versus [DNA] gave the value of K_b. When measuring the absorption spectra, an equal amount of CT-DNA was added to both the test solution (2.5 ml of Tris +25 μl of stock solution of test compound) and the reference solution (2.5 ml of Tris +25 μl of DMF) to eliminate the absorption of CT-DNA itself.

2.4.2 | Competitive binding with EB

The extent of fluorescence quenching of EB bound to CT-DNA can be used to determine the extent of binding between an additional molecule and CT-DNA.[24] The competitive binding experiments were carried out in buffer

TABLE 1 Crystal data and structure refinement for complexes **1** and **2**

	1	2
Empirical formula	$C_{60}H_{52}Ag_2N_{10}O_8$	$C_{30}H_{32}Ag_2N_4O_5$
Formula weight	1256.86	744.34
Crystal system	Monoclinic	Monoclinic
Space group	P2(1)/c	C2/c
a (Å)	11.532(2)	19.913(11)
b (Å)	15.374(3)	8.807(5)
c (Å)	35.824(7)	16.437(10)
α (°)	90	90
β (°)	92.300(3)	92.084(7)
γ (°)	90	90
V (Å$^{3)}$	6346(2)	2881(3)
Z	4	4
ρ_{calcd} (mg m^{-3})	1.315	1.716
μ (mm^{-1})	0.674	1.406
F[000]	2560	1496
Crystal size (mm^3)	0.40 × 0.38 × 0.30	0.40 × 0.38 × 0.30
$h/k/l$ (max., min.)	$-13 \le h \le 12$, $-18 \le k \le 18$, $-43 \le l \le 41$	$-23 \le h \le 24$, $-10 \le k \le 10$, $-19 \le l \le 16$
θ range for data collection (°)	1.44 to 25.50	2.05 to 25.50
Goodness-of-fit on F^2	1.036	1.069
Final R_1, wR_2 indices [$I > 2\sigma(I)$]	$R_1 = 0.0451$, $wR_2 = 0.1163$	$R_1 = 0.0516$, $wR_2 = 0.1418$
R_1, wR_2 indices (all data)	$R_1 = 0.0669$, $wR_2 = 0.1235$	$R_1 = 0.0627$, $wR_2 = 0.156$
Largest differences, peak and hole (e Å^{-3})	0.432 and −0.432	1.693 and −0.959

TABLE 2 Selected bond lengths (Å) and bond angles (°) of Ag(I) complexes **1** and **2**

Complex 1				
Bond distances	Ag(1)–N(5)	2.115(3)	Ag(1)–N(2)	2.121(3)
	Ag(1)–Ag(2)	3.0450(6)	Ag(2)–N(7)	2.153(3)
	Ag(2)–N(3)	2.157(3)		
Bond angles	N(5)–Ag(1)–N(2)	172.36(12)	N(5)–Ag(1)–Ag(2)	94.13(9)
	N(2)–Ag(1)–Ag(2)	86.20(9)	N(7)–Ag(2)–N(3)	156.33(12)
	N(3)–Ag(2)–Ag(1)	84.42(8)	N(7)–Ag(2)–Ag(1)	78.65(9)
	C(7)–N(5)–Ag(1)	128.8(3)	C(1)–N(5)–Ag(1)	124.5(3)
	C(32)–N(3)–Ag(2)	130.2(2)	C(38)–N(3)–Ag(2)	123.8(3)
	C(22)–N(7)–Ag(2)	125.4(3)	C(21)–N(7)–Ag(2)	128.0(3)
	C(51)–N(2)–Ag(1)	125.6(3)	C(52)–N(2)–Ag(1)	127.8(2)
Complex **2**				
Bond distances	Ag(1)–N(1)	2.274(5)	Ag(1)–C(9)#2	2.353(6)
	Ag(1)–O(2)#1	2.330(5)	Ag(1)–C(8)#2	2.426(5)
	Ag(1)–O(2)	2.330(5)	Ag(1)–O(2)#3	2.540(6)
	O(2)–Ag(1)#3	2.540(6)	C(8)–Ag(1)#4	2.426(5)
	C(9)–Ag(1)#4	2.353(6)		
Bond angles	N(1)–Ag(1)–O(2)#1	104.01(18)	N(1)–Ag(1)–O(2)	104.01(18)
	N(1)–Ag(1)–C(9)#2	111.7(2)	O(2)#1–Ag(1)–C(9)#2	144.2(2)
	O(2)–Ag(1)–C(9)#2	144.2(2)	N(1)–Ag(1)–C(8)#2	143.8(2)
	O(2)#1–Ag(1)–C(8)#2	111.9(2)	O(2)–Ag(1)–C(8)#2	111.9(2)
	C(9)#2–Ag(1)–C(8)#2	32.6(2)	N(1)–Ag(1)–O(2)#3	101.30(18)
	O(2)#1–Ag(1)–O(2)#3	78.7(2)	O(2)–Ag(1)–O(2)#3	78.7(2)
	C(9)#2–Ag(1)–O(2)#3	93.8(2)	C(8)#2–Ag(1)–O(2)#3	90.55(19)
	C(10)–N(1)–Ag(1)	128.1(4)	C(1)–N(1)–Ag(1)	126.0(4)
	C(12)–O(2)–Ag(1)	103.2(4)	C(12)–O(2)–Ag(1)#3	137.4(4)
	Ag(1)–O(2)–Ag(1)#3	100.7(2)	C(9)–C(8)–Ag(1)#4	70.7(3)
	C(7)–C(8)–Ag(1)#4	108.5(4)	C(8)–C(9)–Ag(1)#4	76.7(4)

by keeping [DNA]/[EB] = 1.13 and varying the concentrations of the compounds. The fluorescence spectra of EB were measured using an excitation wavelength of 520 nm and the emission range was set between 550 and 750 nm. The spectra were analyzed according to the classical Stern–Volmer equation[25]:

$$\frac{I_0}{I} = 1 + K_{SV}[Q] = 1 + K_q\tau_0[Q]$$

where I_0 and I are the fluorescence intensities at 599 nm in the absence and presence of the quencher, respectively, K_{SV} is the linear Stern–Volmer quenching constant, [Q] is the concentration of the quencher, K_q is the quenching rate constant and τ_0 is luminescence decay time in the absence of the quencher. In these experiments, [CT-DNA] = 2.5×10^{-3} M and [EB] = 2.2×10^{-3} M.

2.4.3 | Viscosity titration measurements

Viscosity experiments were conducted with an Ubbelohde viscometer, immersed in a water bath maintained at 25.0 ± 0.1 °C. Titrations were performed for each complex (3 μM), and each was introduced into CT-DNA solution (50 μM) present in the viscometer. Data were analyzed as $(\eta/\eta_0)^{1/3}$ versus the ratio of the concentration of the compound to CT-DNA, where η is the viscosity of CT-DNA in the presence of the compound and η_0 is the viscosity of CT-DNA alone. Viscosity values were calculated from the observed flow times of CT-DNA-containing solutions corrected for the flow time of buffer alone (t_0): $\eta = (t - t_0)$.[26]

3 | RESULTS AND DISCUSSION

3.1 | Characterization of complexes

The free ligands bobb and aobb and the Ag(I) complexes are stable in both air and solution environments. The syntheses of complexes **1** and **2** were carried out in the dark to avoid photodecomposition. The Ag(I) complexes are soluble in DMF and dimethylsulfoxide, and partially soluble in water and other organic solvents such as methanol, ethanol, acetone, petroleum ether, trichloromethane, etc. The results of elemental analyses show that the composition of complex **1** is $[Ag_2(bobb)_2]\cdot(NO_3)_2$ and **2** is $[Ag_2(crotonate)_2(aobb)]_n$. The molar conductance values show that complex **1** is a 1:2 electrolyte, while complex **2** is a nonelectrolyte in DMF.[27]

The IR spectra of the free ligand bobb and its Ag(I) complex **1** were compared. Free bobb exhibits a characteristic C═N stretching frequency at 1496 cm^{-1}, while the C═N stretching band of the complex is observed at 1548 cm^{-1}. Hence, the C═N stretching frequencies are shifted upon complexation,[28] indicating that the nitrogen atoms of the ligand are coordinated to the Ag(I) center. Similar shifts also appear in the spectrum of complex **2**, which lead to the same conclusion. A strong, fairly broad absorption at 1382 cm^{-1} indicates that ionic nitrate groups (D_{3h}) are present in complex **1**.[29,30] Since the carboxylate group can coordinate to the metal ion in a bidentate bridging, a bidentate chelating or a monodentate fashion, the 'Δ criterion', which is based on the difference between the ν_{as}(COO) and ν_{s}(COO) values, compared to the corresponding value in sodium carboxylate, is currently employed to determine the coordinating mode of carboxylate group.[31,32] The ν_{as}(COO) is assigned to the strong bands at 1549 (**2**) and 1540 cm^{-1} (sodium crotonate) whereas the ν_{s}(COO) is attributed to the 1402 (**2**) and 1389 cm^{-1} (sodium crotonate) peaks. The data suggest that crotonate groups in complex **2** behave as bidentate bridging ligands.[33,34] This conclusion is confirmed by the result of the crystal structure analysis.

DMF solutions of ligands and Ag(I) complexes show, as expected, almost identical UV spectra. In the UV–visible spectra, the band observed for free bobb is marginally red-shifted by 6 nm in the spectrum of complex **1**, again showing coordination of the C═N group to the Ag(I) center. The absorption bands at 280 nm are assigned to π–π* (imidazole) transition.[35–37] Analogously, the UV bands of aobb (279, 287 nm) are also marginally red-shifted by about 1 nm in the spectrum of complex **2**. This phenomenon also shows that C═N is involved in coordination to the metal center.

3.2 | Description of structures

3.2.1 | Crystal structure of complex 1

The crystal structure of complex **1** consists of a binuclear $[Ag_2(bobb)_2]^{2+}$ motif and two NO_3^- anions per formula unit. The Ag(I) atom displays a trigonal planar coordination structure consisting of three nitrogen atoms from two bobb ligands. In addition, the coordination geometry between two Ag(I) atoms indicates strong interaction (Ag···Ag = 3.080(0) Å),[38,39] as shown in Figure 1. In complex **1**, the two benzimidazole rings belonging to the different ligands result in intramolecular π···π interactions (centroid-to-centroid distance, d = 3.615 Å).[40]

As shown in Figure 2, there are two kinds of conjugated effect between the units, which are between imidazole ring and benzyl π···π interactions ((i) d = 3.602(0) Å; (ii) d = 3.683(0) Å) and make the crystal structure more stable. These conjugated effects generate an infinite two-dimensional layer.

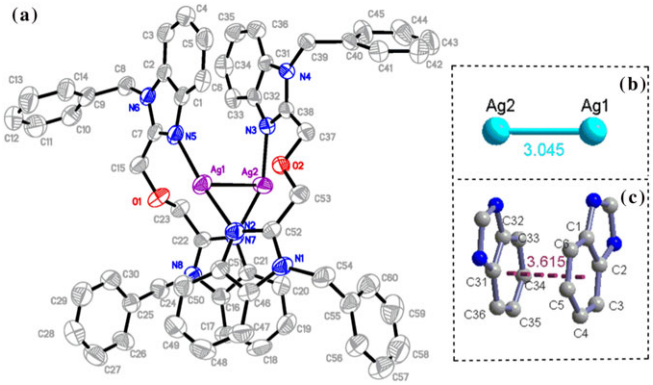

FIGURE 1 (a) molecular structure of complex **1** with displacement ellipsoids drawn at the 30% probability level. The counter anions and hydrogen atoms are omitted for clarity. (b) distance between the two Ag(I) centers is 3.045(0) Å. (c) the π···π interactions between two benzimidazole rings from the same units, d = 3.615(2) Å

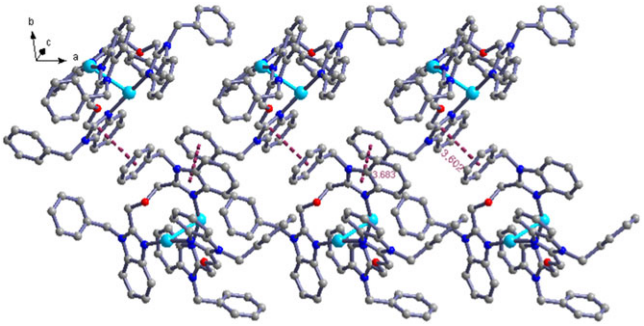

FIGURE 2 Structure of the complex **1** linked via π–π stacking interactions (dashed lines)

3.2.2 | Crystal structure of complex 2

Complex **2** possesses two crystallographically unique Ag(I) atoms, one aobb ligand and two crotonate anions, where the component moieties all lie in general positions with no crystallographically imposed symmetry (Figure 3). Complex **2** is a unique metal organic compound. The free ligand aobb is a bridging ligand. It is not only a σ-bonding ligand, but also a π-acid ligand. The adjacent Ag(I) centers are bridged by allyl from aobb. Ag1 and Ag2 have the same coordination environments, which are five-coordinated by two oxygen atoms from two crotonate anions (Ag(1)–O(2)#1 = 2.331(5) Å, Ag(1)–O(2)#3 = 2.539(6) Å), one nitrogen atom from one aobb ligand (Ag–N = 2.274(5) Å) and two carbon atoms from one allyl(aobb) (C(57)–Ag(1)#4 = 2.430(5) Å and C(58)–Ag(1)#4 = 2.353(6) Å). Moreover, Ag1, Ag2, O(2)#1 and O(2)#3 are connected and form a parallelogram. Different from the structure of **1**, in complex **2**, the adjacent Ag(I) centers are bridged by allyl from aobb to form

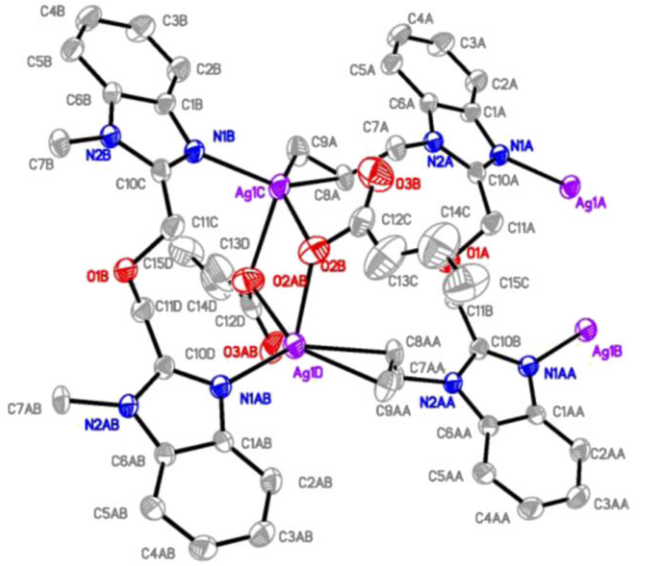

FIGURE 3 Environment of the Ag(I) cation in complex **2** showing 30% thermal probability ellipsoids. The hydrogen atoms are omitted for clarity

—Ag—aobb—Ag0— chains, which are extended into two-dimensional frameworks through strong π–π interactions (d = 3.536(2) Å), as shown in Figures 4 and 5. In addition, hydrogen bonds (C—H···O) also contribute to the stability of the structure.

3.3 | DNA binding properties

3.3.1 | Electronic absorption titration

The electronic absorption spectra of the Ag(I) complexes in the absence and presence of CT-DNA are shown in Figure 6. As can be seen, there is a band at 275 nm. Upon addition of increasing CT-DNA concentrations, these bands exhibit hypochromism of 38.1 and 68.2%, respectively. From the electronic absorption spectroscopy experiments, K_b values of complexes **1** and **2** are 6.28×10^5 and 7.61×10^5 M^{-1}, respectively, as shown in Figure 6(c) and (d). Comparing the molecular structures of the two complexes, we suggest that their binding affinities follow the order: **2** > **1**. The charge transfer of coordinated ligands resulting from coordination to the Ag(I) atom should reduce the charge density of the planar conjugate system, which is conducive to intercalation.[35,41] This difference in the DNA binding ability could also be attributed to the presence of an electron-deficient center in the Ag(I) complexes, allowing an additional interaction between the complexes and phosphate-rich DNA backbone compared to the free ligand.[42–44]

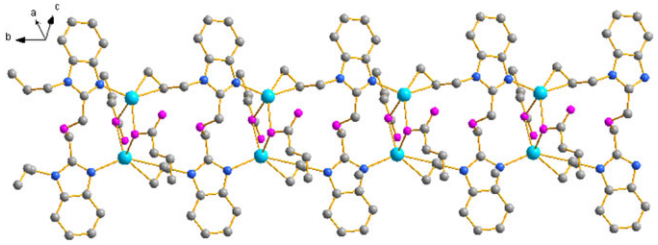

FIGURE 4 Polymer chain structure of complex **2**

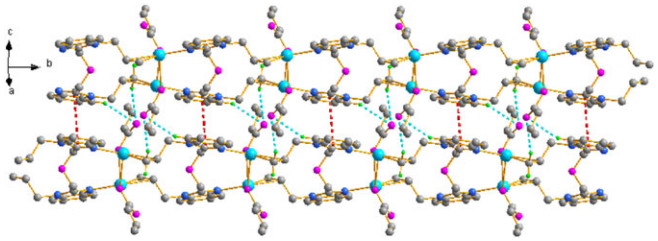

FIGURE 5 Infinite two-dimensional supramolecular layer formed via π–π interactions and C—H···Ag hydrogen bonding in complex **2**

3.3.2 | Fluorescence spectra

EB does not show any appreciable emission in buffer solution due to fluorescence quenching by the solvent. Upon addition of complex to a solution containing EB, no change in the fluorescence spectra is observed. However, the fluorescence intensity of EB is greatly enhanced upon addition of CT-DNA, due to its strong intercalation with the DNA base pairs. Addition of a second molecule, which may bind to DNA more strongly than EB, can the result in a decrease the DNA-induced EB emission by displacement of EB.[45]

The addition of the complexes results in a significant decrease of the intensity of the emission band of the DNA–EB system at 595 nm, indicating competitive binding of the compounds to DNA. The Stern–Volmer plots (Figure 7) show that the fluorescence quenching of EB bound to DNA by the two complexes follows a linear relationship, consistent with intercalation of the test compounds. The K_{SV} values for complexes **1** and **2** are $(3.65 \pm 0.15) \times 10^3$ and $(6.40 \pm 0.22) \times 10^3$ M^{-1}, respectively. Moreover, the K_q values for complexes **1** and **2** are 3.65×10^{11} and 6.40×10^{11} M^{-1} s^{-1}, which are far larger than 2.0×10^{10} M^{-1} s^{-1}, the maximum diffusion collision quenching rate constant of various quenchers with the biopolymer. Consequently, the probable mechanism of fluorescence quenching of complexes **1** and **2** binding reactions should follow a static quenching process rather than a dynamic one.[46] To a certain extent, reduction of the emission intensity at 595 nm gives a measure of the binding propensity of the complexes to CT-DNA. The phenomena suggest that the complexes can compete for DNA binding sites with EB and displace EB from the EB–DNA system,[47] which is usually characteristic of the intercalative interaction of compounds with DNA.[48] Moreover, the binding strengths of the complexes follow the same order as from the UV–visible experiments.

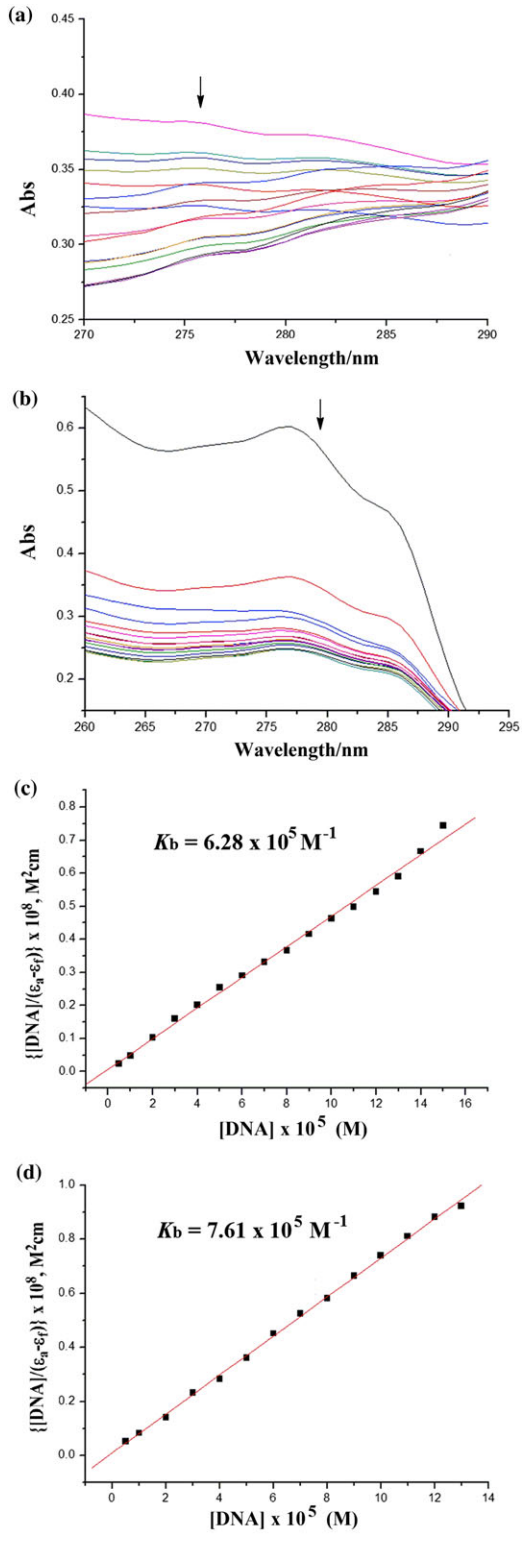

FIGURE 6 Electronic spectra of (a) complex **1** and (b) complex **2** in Tris–HCl buffer upon addition of CT-DNA. The arrow shows the emission intensity changes with increasing DNA concentration. [DNA]/($\varepsilon_a - \varepsilon_f$) versus [DNA] for the titration of (c) complex **1** and (d) complex **2** with CT-DNA

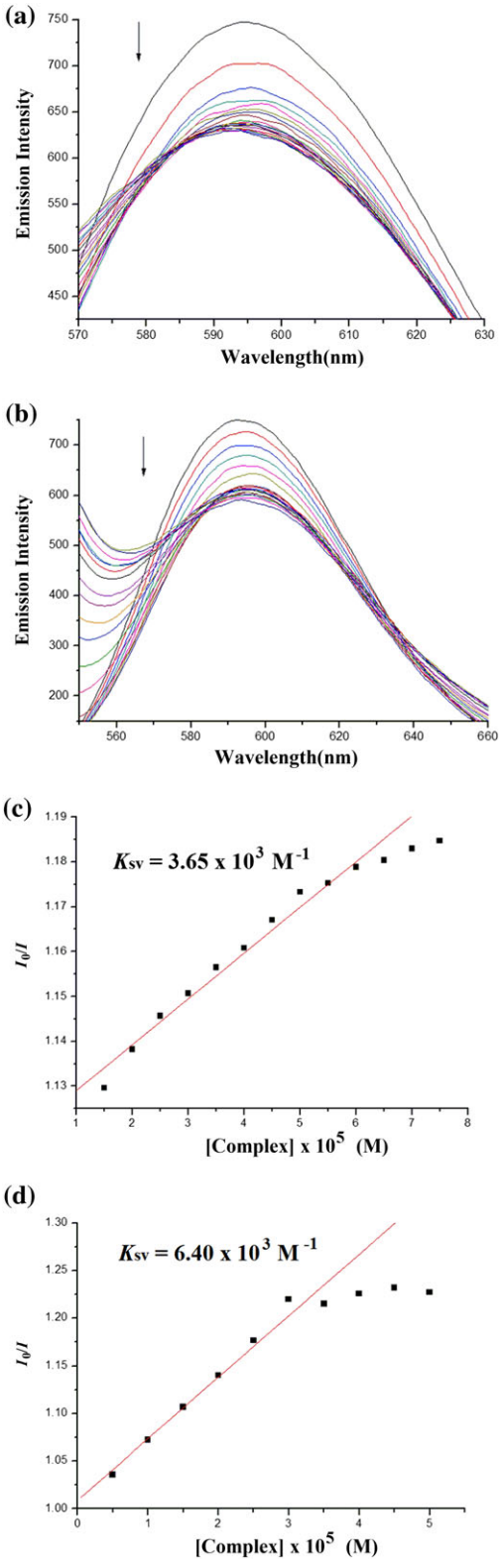

FIGURE 7 Emission spectra of EB bound to CT-DNA in the presence of (a) complex **1** and (b) complex **2** (λ_{ex} = 596 nm). The arrows show the intensity changes with increasing concentration of the complexes. Fluorescence quenching curves of EB bound to CT-DNA by (c) complex **1** and (d) complex **2**. (plots of I_0/I versus [complex])

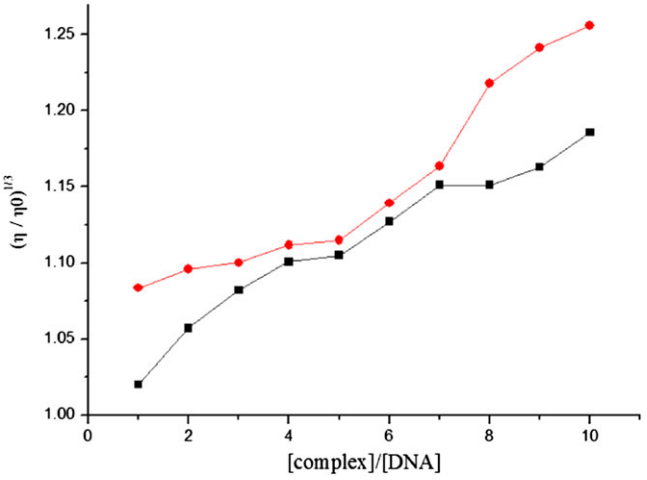

FIGURE 8 Effect of increasing amounts of compounds on relative viscosity of DNA at 25.0 ± 0.1 °C

3.3.3 | Viscosity measurements

Finally, we used viscosity measurements to probe the interactions of the two complexes with DNA. For complexes **1** and **2**, as increasing amounts are added, the viscosity of DNA increases steadily (Figure 8). In classical intercalation, the DNA helix lengthens as base pairs are separated to accommodate the bound ligand, leading to increased DNA viscosity; whereas a partial, non-classical ligand intercalation causes a bend (or kink) in the DNA helix, reducing its effective length and thereby its viscosity.[49] Hence, these results provide further evidence that the two complexes intercalate with CT-DNA[45] and the DNA binding affinities follow the order: **2** > **1**, which is consistent with the absorption and fluorescence spectral results discussed above.

For this difference, we attribute possible reasons. By comparison of the molecular structure of the Ag(I) complexes, we find their DNA binding ability also could be attributed to the presence of where an additional interaction between the complex and phosphate-rich DNA backbone may occur with an electron-deficient center in the charged Ag(I) complexes. Substituents are not the same in the ligands, resulting in electron density changes. In addition, the reason for the difference in the binding strength for two Ag(I) complexes can be attributed to the difference in steric hindrance and electron density, which are both caused by the introduction of substituents and geometric structure.

4 | CONCLUSIONS

Two Ag(I) complexes with different flexible bis(benzimidazole) ligands have been prepared and structurally characterized. Complex **2** is a unique metal organic compound. The results indicate that the flexible bis(benzimidazole) ligands have important effects on the Ag solid structures. DNA binding studies indicate that the investigated complexes bind to DNA via an intercalation binding mode. The Ag(I) complexes can insert and stack between the DNA base pairs more easily; especially, complex **2** can bind to DNA more strongly than complex **1**. This is due to the chelating effects which can enhance the planar functionality of the metal complexes. These results demonstrate the usefulness of Ag(I) complexes in the design of new functional materials with an impressive range of potential applications, including new antitumor drugs.

ACKNOWLEDGMENTS

The research presented was supported by the National Natural Science Foundation of China (grant no. 21367017).

REFERENCES

[1] R. A. Haque, M. Z. Ghdhayeb, S. Budagumpi, A. W. Salman, M. B. Khadeer Ahamed, A. M. S. A. Majid, *Inorg. Chim. Acta* **2013**, *394*, 519.

[2] T. Fuente, M. Martın-Fontecha, J. Sallander, B. Benhamu, M. Campillo, R. A. Medina, L. P. Pellissier, S. Claeysen, A. Dumuis, L. Pardo, M. L. Lopez-Rodrıguez, *J. Med. Chem.* **2010**, *53*, 1357.

[3] O. Dogan, S. Demir, I. Ozdemir, B. Cetinkaya, *Appl. Organometal. Chem.* **2011**, *25*, 163.

[4] B. Willis, D. P. Arya, *Biochem.* **2010**, *49*, 452.

[5] M. J. Clarke, *Coord. Chem. Rev.* **2002**, *232*, 69.

[6] C. G. Hartinger, S. Zorbas-Seifried, M. A. Jakupec, B. Kynast, H. Zorbas, B. K. Keppler, *J. Inorg. Biochem.* **2006**, *100*, 891.

[7] G. Sathyaraj, T. Weyhermller, B. U. Nair, *Eur. J. Med. Chem.* **2010**, *45*, 284.

[8] C. Metcalfe, J. Thomas, *Chem. Soc. Rev.* **2003**, *32*, 215.

[9] R. Blasius, C. Moucheron, A. K. Mesmasker, *Eur. J. Inorg. Chem.* **2004**, 3971.

[10] T. Sun, K. Seff, *Chem. Rev.* **1994**, *94*, 857.

[11] I. Rabin, W. Schulze, *J. Phys. Chem. B.* **2004**, *108*, 14575.

[12] C. A. Tsipis, E. E. Karagiannis, P. F. Kladou, A. C. Tsipis, *J. Am. Chem. Soc.* **2004**, *126*, 12916.

[13] A. N. Khlobystov, A. J. Blake, N. R. Champness, D. A. Lemenovskii, A. G. Majouga, N. V. Zyk, M. Schroder, *Coord. Chem. Rev.* **2001**, *222*, 155.

[14] D. J. Eisler, R. J. Puddephatt, *Inorg. Chem.* **2006**, *45*, 7295.

[15] H. J. Hao, D. Sun, Y. H. Li, F. J. Liu, R. B. Huang, L. S. Zheng, *Cryst. Growth Des.* **2011**, *11*, 3564.

[16] M. Sanchez-Moreno, E. Entrala, D. Janssen, J. M. Salas-Peregrin, A. Osuna, *Pharmacol.* **1996**, *52*, 61.

[17] Z. Y. Yang, Y. Wang, Y. Wang, *Bioorg. Med. Chem. Lett.* **2007**, *17*, 2096.

[18] G. L. Pan, Y. C. Bai, H. Wang, J. Kong, F. R. Shi, Y. H. Zhang, X. L. Wang, H. L. Wu, *Z. Naturforsch. B.* **2013**, *68*, 257.

[19] H. L. Wu, R. R. Yun, K. T. Wang, K. Li, X. C. Huang, T. Sun, *Z. Anorg. Allg. Chem.* **2010**, *636*, 629.

[20] H. L. Wu, F. Kou, F. Jia, B. Liu, J. K. Yuan, Y. Bai, *Z. Anorg. Allg. Chem.* **2012**, *638*, 44.

[21] Bruker, APEX2 and SAINT, Bruker AXS Inc., Madison, WI, **2007**.

[22] G. M. Sheldrick, *SHELXTL*, Siemens Analytical X-ray Instruments Inc., Madison, WI **1996**.

[23] P. X. Xi, Z. H. Xu, X. H. Liu, F. H. Chen, Z. Z. Zeng, X. W. Zhang, Y. Liu, *J. Fluoresc.* **2009**, *19*, 63.

[24] G. F. Qi, Z. Y. Yang, D. D. Qin, B. D. Wang, T. R. Li, *Chem. Pharm. Bull.* **2008**, *56*, 452.

[25] J. R. Lakowicz, G. Webber, *Biochem.* **1973**, *12*, 4161.

[26] C. P. Tan, J. Liu, L. M. Chen, S. Shi, L. N. Ji, *J. Inorg. Biochem.* **2008**, *102*, 1644.

[27] W. J. Geary, *Coord. Chem. Rev.* **1971**, *7*, 81.

[28] W. K. Dong, Y. X. Sun, G. H. Liu, L. Li, X. Y. Dong, X. H. Gao, *Transit. Metal Chem.* **2012**, *638*, 1370.

[29] P. S. Subramanian, P. C. Dave, V. P. Boricha, D. Srinivas, *Polyhedron* **1998**, *17*, 443.

[30] L. K. Thompson, B. S. Ramaswamy, R. D. Dawe, *Can. J. Chem.* **1978**, *56*, 1311.

[31] K. Nakamoto, *Infrared and Raman Spectra of Inorganic and Coordination Compounds*, John Wiley, New York **1978**.

[32] J. Catterick, P. Thornton, *Adv. Inorg. Chem.* **1977**, *20*, 291.

[33] Y. Y. Wang, Q. Shi, Q. Z. Shi, Y. C. Gao, Z. Y. Zhou, *Polyhedron* **1999**, *18*, 2009.

[34] H. L. Wu, J. G. Liu, P. Liu, W. B. Lv, B. Qi, X. K. Ma, *J. Coord. Chem.* **2008**, *61*, 1027.

[35] L. K. Thompson, B. S. Ramaswamy, E. A. Seymour, *Can. J. Chem.* **1977**, *55*, 878.

[36] H. L. Wu, J. K. Yuan, Y. Bai, G. L. Pan, H. Wang, J. Kong, X. Y. Fan, H. M. Liu, *Dalton Trans.* **2012**, *41*, 8829.

[37] H. L. Wu, B. Liu, F. Kou, F. Jia, J. K. Yuan, Y. Bai, *J. Chin. Chem. Soc. Taip.* **2012**, *5*, 836.

[38] K. N. Power, T. L. Hennigar, M. J. Zaworotko, *New J. Chem.* **1998**, *22*, 177.

[39] O. M. Yaghi, H. J. Li, *J. Am. Chem. Soc.* **1996**, *118*, 295.

[40] C. L. Chen, C. Y. Su, Y. P. Cai, H. X. Zhang, A. W. Xu, B. S. Kang, Z. L. Hans-Conrad, *Inorg. Chem.* **2003**, *42*, 3738.

[41] H. L. Wu, K. T. Wang, B. Liu, F. Kou, F. Jia, J. K. Yuan, Y. Bai, *Inorg. Chim. Acta* **2012**, *384*, 302.

[42] R. Indumathy, T. Weyhermüller, B. U. Nair, *Dalton. Trans.* **2010**, *39*, 2087.

[43] M. Shakir, M. Azam, M. F. Ullah, S. M. Hadi, *J. Photochem. Photobiol. B* **2011**, *104*, 449.

[44] H. L. Wu, J. K. Yuan, Y. Bai, G. L. Pan, H. Wang, X. B. Shu, *J. Photochem. Photobiol. B.* **2012**, *107*, 65.

[45] R. F. Pasternack, M. Caccam, B. Keogh, T. A. Stephenson, A. P. Williams, F. J. Gibbs, *J. Am. Chem. Soc.* **1991**, *113*, 6835.

[46] Q. H. Zhou, P. Yang, *Acta Chim. Sin.* **2006**, *64*, 793.

[47] Y. B. Zeng, N. Yang, W. S. Liu, N. Tang, *J. Inorg. Biochem.* **2003**, *97*, 258.

[48] C. V. Kumar, J. K. Barton, N. J. Turro, *J. Am. Chem. Soc.* **1985**, *107*, 5518.

[49] S. Satyanarayana, J. C. Dabroniak, J. B. Chaires, *Biochem.* **1992**, *31*, 9319.

SUPPORTING INFORMATION

Additional Supporting Information may be found online in the supporting information tab for this article.

How to cite this article: Mao S, Shen K, Shi X, Xu Y, Wu H. Two silver(I) complexes with bis(benzimidazole)-2-oxopropane ligands: Syntheses, crystal structures and DNA binding studies. *Appl Organometal Chem*. 2017;e3747. https://doi.org/10.1002/aoc.3747